

Title	Development of nanostructured, stress-free Co-rich CoPtP films for magnetic microelectromechanical system applications
Authors	Kulkarni, Santosh;Roy, Saibal
Publication date	2007-05-08
Original Citation	Kulkarni, S. and Roy, S. (2007) 'Development of nanostructured, stress-free Co-rich CoPtP films for magnetic microelectromechanical system applications', Journal of Applied Physics, 101(9), pp. 09K524. doi: 10.1063/1.2712032
Type of publication	Article (peer-reviewed)
Link to publisher's version	http://aip.scitation.org/doi/abs/10.1063/1.2712032 - 10.1063/1.2712032
Rights	© 2007 American Institute of Physics, This article may be downloaded for personal use only. Any other use requires prior permission of the author and AIP Publishing. The following article appeared in Kulkarni, S. and Roy, S. (2007) 'Development of nanostructured, stress-free Co-rich CoPtP films for magnetic microelectromechanical system applications', Journal of Applied Physics, 101(9), pp. 09K524 and may be found at http://aip.scitation.org/doi/abs/10.1063/1.2712032
Download date	2024-04-20 03:05:31
Item downloaded from	https://hdl.handle.net/10468/4228



UCC

University College Cork, Ireland
Coláiste na hOllscoile Corcaigh

Development of nanostructured, stress-free Co-rich CoPtP films for magnetic microelectromechanical system applications

Santosh Kulkarni and Saibal Roy

Citation: *Journal of Applied Physics* **101**, 09K524 (2007); doi: 10.1063/1.2712032

View online: <http://dx.doi.org/10.1063/1.2712032>

View Table of Contents: <http://aip.scitation.org/toc/jap/101/9>

Published by the *American Institute of Physics*

AIP | Journal of
Applied Physics

Save your money for your research.
It's now **FREE** to publish with us -
no page, color or publication charges apply.

Publish your research in the
Journal of Applied Physics
to claim your place in applied
physics history.

Development of nanostructured, stress-free Co-rich CoPtP films for magnetic microelectromechanical system applications

Santosh Kulkarni and Saibal Roy^{a)}

Energy Processing for ICT Group, Tyndall National Institute, Cork, Ireland

(Presented on 9 January 2007; received 1 November 2006; accepted 18 December 2006; published online 8 May 2007)

Co-rich CoPtP alloys have been electrodeposited using direct current (dc) and pulse-reverse (PR) plating techniques. The surface morphology, crystalline structure, grain size, and magnetic properties of the plated films have been compared. The x-ray analysis and magnetic measurements reveal the presence of Co hcp hard magnetic phase with *c* axis perpendicular to the substrate for dc and in plane for PR plated films. The dc plated films have a granular structure in the micron scale with large cracks, which are manifestation of stress in the film. Only by using a combination of optimized PR plating conditions and stress relieving additive, we are able to produce 1–6 μm thick (for 1 hour of plating), stress-free, and nanostructured (~ 20 nm) Co-rich CoPtP single hcp phase at room temperature, with an intrinsic coercivity of 1500 Oe. © 2007 American Institute of Physics. [DOI: 10.1063/1.2712032]

With the progress in the field of magnetic microelectromechanical system (MEMS) technologies^{1–5} there has been growing interest in developing electroplated, nanostructured hard magnetic materials^{6,7} for microactuators, micromotors, microswitches, etc. The possibility of these electroplated materials, retaining hard magnetic properties up to several microns in thickness, gives researchers opportunity to explore them for microfabrication of MEMS devices. Recently, we reported^{8,9} the design and simulation of different electromagnetic power generators using electroplated equiatomic face centered tetragonal (fct) phase CoPt micromagnets.

It is known that Co-rich Co₈₀Pt₂₀P films exhibit large energy products in their as-deposited state due to the high anisotropy induced by the incorporation of Pt in the hexagonal close-packed (hcp) phase of Co.^{10,11} Even though the Co-rich CoPtP has lower magnetic properties compared to the fct phase CoPt and FePt films, they do not require high temperature annealing, making them an attractive option for magnetic MEMS devices. Previous works^{12,13} have demonstrated the use of electroplating technique for deposition of Co-rich CoPt films, having a single hcp phase. They reported electroplated films with large coercivities of 6 kOe for a thickness up to 1 μm .

In the present work, we compare different electroplating techniques such as direct current (dc) and pulse-reverse (PR) plating with and without additives to produce relatively thick, stress-free, nanostructured Co-rich CoPtP film while improving their magnetic properties.

The Co-rich CoPtP films were galvanostatically deposited using a bath,⁶ with 0.1M of cobalt-sulphamate, 10 mM of Pt P-salt, 0.1M of dibasic ammonium citrate, 0.1M glycine, and 0.1M of sodium hypophosphate. The pH of the solution was adjusted to 8 by adding sodium hydroxide. Co pieces were used as anode and silicon wafer with sputtered Cu/Ti seed layer was used as cathode. The electrolyte was

divided into two parts. One part was used for depositing films using dc plating at current densities varying from 15 to 20 mA/cm² at room temperature, 40 mA/cm² at 40 °C, and 50 mA/cm² at 60 °C. To the second part of the electrolyte, 4.5 g/l of stress relieving additive, saccharin, was added. The second set of films was deposited by PR plating using bath with saccharin at same condition as in dc plating. In PR plating, amplitude for forward and reverse pulses and their duty cycles were varied to get the optimized structure and coercivity. The surface morphology and composition of different plated films were characterized using scanning electron microscopy (SEM) and energy dispersive x ray (EDX), respectively. The thickness of each of the plated films was measured by DekTak thickness profilometer. The crystalline phase and grain size were determined using Philips X'pert x-ray diffractometer (XRD) with Cu *K* α radiation (40 kV, 50 mA). In-plane and out-of-plane magnetic properties were measured in Quantum Design SQUID magnetometer (MPMS-XL5) with a maximum applied field of 5 T.

The first set of films was electrodeposited in dc plating using the bath without saccharin. In order to optimize the plating conditions, the films were plated at different current densities as described in the previous section. All the films were plated for 1 h. The plated films visually were smooth, shiny, and showed strong adherence to the substrate. The plating rates were around 3 $\mu\text{m}/\text{h}$ at room temperature, 4 $\mu\text{m}/\text{h}$ at 40 °C, and 6 $\mu\text{m}/\text{h}$ at 60 °C. Figure 1(a) shows the SEM image of the film plated at 20 mA/cm² at room temperature, which is typical of all other plated films. The films show a granular structure in the micron scale and appear to be stressed with the presence of large cracks. In the case of conventional dc plating on a highly polished Si wafer substrate having a surface roughness of the order of submicrometer to several nanometers will have a rather flat Nernst diffusion layer across its surface microasperities, i.e., peaks and valleys as opposed to unpolished polycrystalline substrate.² This means a smaller diffusion length from the

^{a)}Author to whom correspondence should be addressed; FAX: +353 214270271; electronic mail: saibal.roy@tyndall.ie

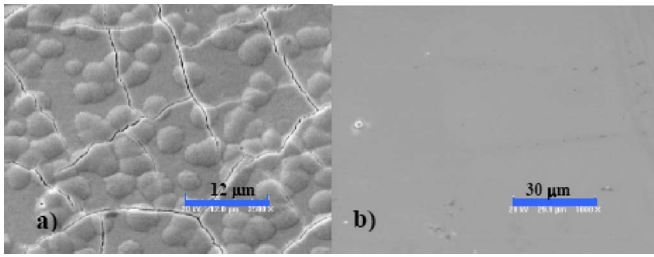


FIG. 1. (Color online) SEM image of film (a) dc plated at 20 mA/cm^2 at room temperature for 1 h ($3 \mu\text{m}$ thick) and (b) PR plated at 20 mA/cm^2 at room temperature for 1 h ($3 \mu\text{m}$ thick).

peak and larger diffusion length from the valley for a depositing ion, giving rise to a relatively higher metal ion concentration and hence greater deposition rate at the peaks than the valleys. This was evident when we dc plated on Si substrate with sputtered Cu/Ti seed layer, as can be seen from Fig. 1(a), which shows preferential growth of metals at different places, causing stress in the film.

To avoid these preferential growths and consequent stress while maintaining a uniform composition and thickness, we employed pulse-reverse technique,² which involves sending a wave form combining forward and reverse pulses with intermittent off period in the plating bath.

The entire cycle, T ($t_{\text{forward}} + t_{\text{rev}} + 2t_{\text{off}}$), is repeated until the plating time is reached. In general for a shorter cathodic pulse, the Nernst diffusion layer (N_d) becomes thinner with an immediate decrease in electrolyte concentration gradient adjacent to the substrate surface during the off time. The thinner the diffusion layer, the more uniform will be the metal deposition across the microasperities. In this work two intermittent off periods, before and after reverse pulse, were provided to achieve the uniform deposition. But the use of only PR plating without stress relieving additive resulted in a very thin film ($<100 \text{ nm}$ after 1 h of plating) without Co hcp phase. To improve the plating rate for PR films, saccharin was added to the bath. Initially, all the PR plating parameters (reverse pulse amplitude, duty cycles, etc.) were varied to find the optimized plating condition. For this, a set of films was plated at a forward current density (I_{forward}) of 20 mA/cm^2 at room temperature, with the reverse pulse amplitude varying from $0.5I_{\text{forward}}$ to $8I_{\text{forward}}$. Figure 2 shows the variation of coercivity with the reverse pulse amplitude

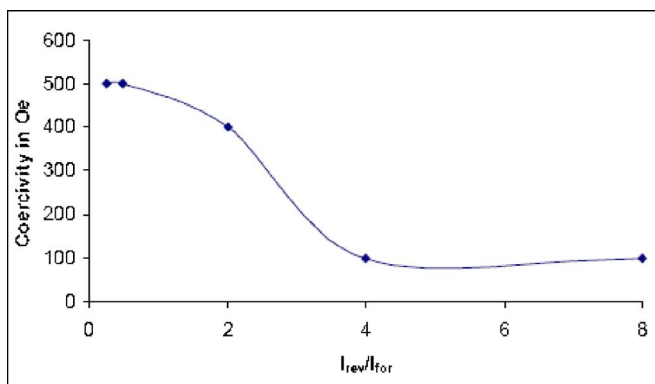


FIG. 2. (Color online) Variation of coercivity with the reverse pulse amplitude as a multiple of forward pulse amplitude.

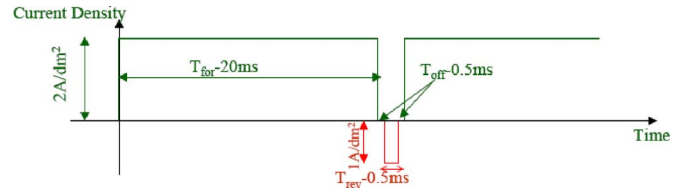


FIG. 3. (Color online) Typical wave form for optimized pulse-reverse (PR) plating.

as a multiple of forward pulse amplitude. Subsequently the reverse pulse amplitude was kept as half of the forward pulse to get a maximum coercivity in the plated films. Similarly, the forward pulse duty cycle was varied from 20 to 100 ms. It was found that a duty cycle of 20 ms is ideal to obtain a composition close to $\text{Co}_{80}\text{Pt}_{20}\text{P}$. The reverse pulse duty cycle and the off times were varied from 0.5 to 2 ms and this variation did not show any effect on the composition of the plated films. The reverse pulse duty cycle and off times were set at 0.5 ms. Figure 3 shows the optimized pulse-reverse wave form for PR plating.

Using the above optimized PR plating parameters and with the addition of saccharin to the plating bath, a second set of films was deposited at 20 mA/cm^2 at room temperature, 40 mA/cm^2 at 40°C , and 50 mA/cm^2 at 60°C . Figure 1(b) shows the SEM image of a PR plated film at 20 mA/cm^2 at room temperature plated for 1 hour, which is

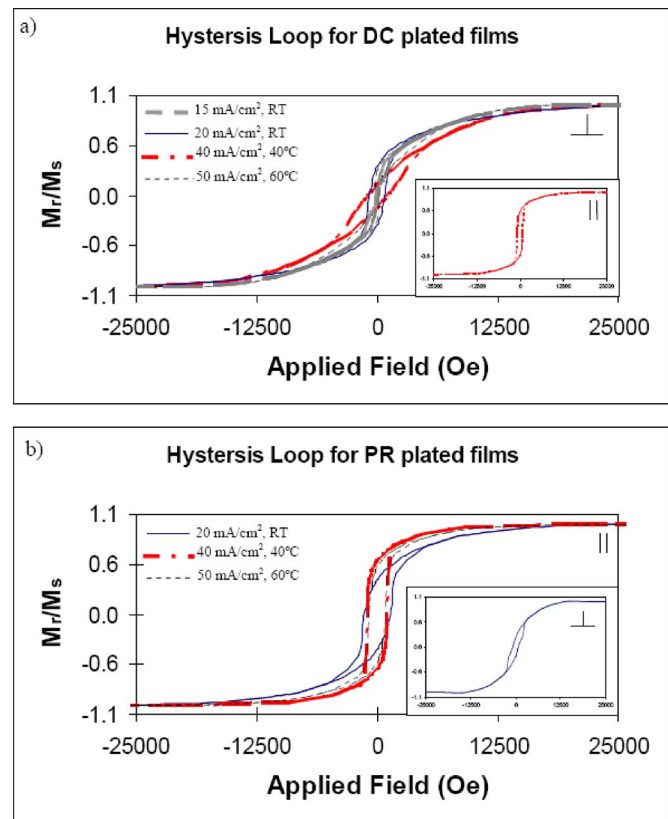


FIG. 4. (Color online) Magnetic measurements for (a) dc plated measurements perpendicular to film plane (inset: in-plane measurements for dc plated film at 40 mA/cm^2 at 40°C) and (b) PR plated films measurements in plane (inset: out-of-plane measurement for PR plated film at 20 mA/cm^2 at RT).

TABLE I. Comparison of different plated films.

Plating technique	Plating conditions	Thickness (μm), 1 hr plating	Phase/peak position	Grain size (nm)	Intrinsic coercivity (Oe) in plane (\parallel) out of plane (\perp)
DC	15 mA/cm ² – room temp	1.5	Amorphous	...	70 (\perp)
DC	20 mA/cm ² – room temp	3	Co hcp phase—40.85°	31.9	800 (\perp)
DC	40 mA/cm ² – 40 °C	4.65	Co hcp phase – 40.95°	25.2	1200 (\perp)
DC	50 mA/cm ² – 60 °C	6.25	Co hcp phase—41.3° & fcc phase—44°	35.4	250 (\perp)
PR	20 mA/cm ² – room temp	3	Co hcp phase—40.8°	20.4	1500 (\parallel)
PR	40 mA/cm ² – 40 °C	4.5	Co hcp phase—41.2°	23.6	1200 (\parallel)
PR	50 mA/cm ² – 60 °C	6.15	Co hcp phase—40.9° & fcc phase—43.9°	25.2	900 (\parallel)

typical of all other PR plated films. The film does not show the presence of any granular structure in the micron scale and stress or cracks. The deposition rates are similar to the ones measured in the dc plating technique despite the contribution of the reverse pulse and off times (t_{off}) towards effective plating current density. This is explained by the increase of throwing power in the bath by the addition of saccharin. The out-of-plane magnetic measurements of the dc plated films are shown in Fig. 4(a), with in-plane measurement for 40 mA/cm² at 40 °C film in the inset, which is typical of other in-plane measurements. On the other hand, in-plane magnetic measurements for PR plated films are shown in Fig. 4(b), with out-of-plane measurement for 20 mA/cm² in the inset, which is typical of other out-of-plane measurements. The dc plated films showed a higher coercivity for out-of-plane measurements, while the PR plated films showed a higher in-plane coercivity. Table I summarizes the plating conditions, crystalline phase, thickness, grain size, and intrinsic coercivity of the dc and PR plated films.

The XRD of the dc plated film at 15 mA/cm² at room temperature shows amorphous phase, resulting in a low intrinsic coercivity of 70 Oe. From XRD patterns of the remaining films, the Co hcp peak positions are close to 41°, which necessarily mean that the compositions for the films are similar. The dc plated film at 50 mA/cm² at 60 °C shows the presence of a strong soft magnetic face-centered cubic (fcc) phase along with the hard magnetic Co hcp phase, which leads to a lower coercivity. In contrast, the XRD pattern of PR plated film at 50 mA/cm² at 60 °C shows that the volume fraction of the soft magnetic fcc phase is reduced and hence has a higher intrinsic coercivity of 900 Oe. The grain sizes for all of the plated films are calculated using Scherrer's equation from the full widths at half maximum (FWHMs) of the Co hcp peak. As the grain size of the plated films approaches the single domain size of Co hcp phase¹⁴ (~10 nm), there is a reduction of cancellation of spins due to random orientation, thereby increasing the anisotropy along the *c* axis, which leads to an increase in coercivity. On comparing the results for different dc and PR plated films we find that as the grain size of the films lowers and approaches to the single domain size, the coercivity increases. This can be seen in the case of the dc plated film at 40 mA/cm² at 40 °C having a smallest grain size of 25.2 nm with a single Co hcp

phase when compared to the other dc plated films and hence a highest intrinsic coercivity of 1200 Oe. Similarly PR plated film at 20 mA/cm² at room temperature, which has a least grain size (20.4 nm) of all the plated films with a single Co hcp phase, shows the highest intrinsic coercivity of 1500 Oe. The ratio of perpendicular to in-plane remanence is 0.54 for PR plated film at 20 mA/cm² and decreases with increasing current density. From Fig. 4, PR plated films have a higher loop squareness ($S_{\text{max}}=0.61$ for film plated at 40 mA/cm² at 40 °C) along with larger intrinsic coercivity, when compared to dc plated films ($S_{\text{max}}=0.33$ for film plated at 20 mA/cm²). This increase in squareness is believed to be arising out of optimized PR plating technique, which increases the in-plane *c*-axis orientation, leading to higher in-plane anisotropy and hence higher squareness.

In this work, we suggest a method of electrodeposition, which involves a combination of PR plating and addition of stress relieving additives such as saccharin, to plate thick, stress-free, and nano-structured Co-rich CoPtP film with an improvement of 25% in the maximum coercivity over DC plated films. A maximum intrinsic in-plane coercivity of 1500 Oe and a maximum ratio of perpendicular to parallel remanence of 0.54 were observed for a PR plated film deposited at 20 mA/cm² at room temperature having a single Co hcp hard magnetic phase with a grain size of 20 nm.

The authors would like to acknowledge the financial support by the European Union Framework 6 STREP project VIBES No. 507911. One of the authors acknowledges Dr. Fernando Rhen for useful discussions.

¹O. Cugat *et al.*, IEEE Trans. Magn. **39**, 3607 (2003).

²S. Roy *et al.*, J. Magn. Magn. Mater. **290–291**, 1524 (2005).

³F. M. F. Rhen *et al.*, J. Appl. Phys. **97**, 113908 (2005).

⁴K. H. Lee *et al.*, J. Appl. Phys. **91**, 8513 (2002).

⁵M. Albrecht *et al.*, Appl. Phys. Lett. **81**, 2875 (2002).

⁶G. Pattanaik *et al.*, J. Electrochem. Soc. **153**, C6 (2006).

⁷H. D. Park *et al.*, J. Appl. Phys. **99**, 08N305 (2006).

⁸S. Kulkarni *et al.*, J. Appl. Phys. **99**, 08P511 (2006).

⁹S. Kulkarni *et al.*, *Proceedings of the IEEE International Magnetic Conference*, INTERMAG-06, San Diego, CA, May 8-12, 2006, pp. 317.

¹⁰J. B. Aboaf *et al.*, IEEE Trans. Magn. **MAG-19**, 1514 (1983).

¹¹N. Kikuchi *et al.*, J. Phys.: Condens. Matter **11**, L485 (1999).

¹²I. Zana *et al.*, J. Magn. Magn. Mater. **292**, 266 (2005).

¹³I. Zana *et al.*, J. Magn. Magn. Mater. **272–276**, 1698 (2004).

¹⁴B. Jiang *et al.*, J. Appl. Phys. **95**, 7115 (2004).